Multi-Basis-Set (TD-)DFT Methods for Predicting Electron Attachment Energies

Guillaume Thiam, Franck Rabilloud

Multi-Basis-Set (TD-)DFT Methods for Predicting Electron Attachment Energies

Guillaume Thiam* and Franck Rabilloud*

Université de Lyon, Université Claude Bernard Lyon 1, CNRS, Institut Lumière Matière, UMR5306, F-69622 Villeurbanne, France

E-mail: guillaume.thiam@univ-lyon1.fr; franck.rabilloud@univ-lyon1.fr

Abstract

The interaction of low-energy electron collisions with molecules may lead to temporary anions via resonant processes. While experimental measurements, e.g. electron transmission spectroscopy or dissociation electron attachment spectroscopy, are efficient to characterize the temporary anions, simulating the electron attachment is still very challenging. Here, we propose a methodology to calculate the resonance energies of the electron attachment using *ab initio* (TD)-DFT calculations together with two different basis sets: a large basis set with diffuse functions to compute the vertical electron affinity, and a smaller one to calculate the excitation energy of the anion. To demonstrate the capabilities and the reliability of this computational approach, 53 resonance energies from 18 molecules are calculated and compared to experimental data.

Graphical TOC Entry

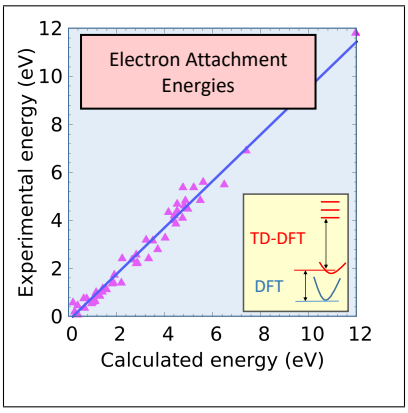

Understanding the interaction of low-energy electron collisions with molecules constitutes a key subject in a large area of fundamental research as well as modern applications in various fields of science such as astrochemistry,[1] radiation-induced damage of biological tissue,[2–4] selective chemistry,[5] or chemical synthesis at nanoscale.[6] Upon the electron collision, the production of a temporary parent anion is expected, the latter being in a metastable state as it lies energetically above the ground state of the neutral molecule.

The capture of the extra electron arises dominantly via shape or core-excited resonances. In the former, the colliding electron is trapped into an empty molecular orbital of the molecule, assuming few influence on the other electrons. Instead, in the case of core-excited resonance, the trapping of the extra electron is concomitant with the promotion of a valence electron in the conduction band.[7] The trapping can also occur with the formation of a dipole-bound anion state via long-range electron interactions with a polar molecule.[8] One of the most efficient mechanism for the induced molecular fragmentation is the Dissociative Electron Attachment (DEA).[9] The scattering electron is captured by the neutral target species to form a transitory negative ion (TNI), which in turn undergoes molecular dissociation into an anion and one or more neutral fragments. Alternatively, the TNI may also eject the excess electron if the dissociation time is longer than the auto-detachment time. Another reaction pathway may lead to the formation of a quasi-stable anion with a very long lifetime.[10]

In experiments, TNIs are usually probed by the Electron Transmission spectroscopy[11,12] (ETS) and the DEA spectroscopy. ETS is used to measure negative electron affinities and study unstable gas-phase anions. Information of the processes immediately after the electron capture mostly relies on the detection of the negative fragments.

A complete theoretical characterization of the temporary anion, which would describe the electron attachment, the relaxation of electronic and vibrational degrees of freedom, and possible fragmentation processes, is still challenging. Limitations come from the difficulty to treat the electron correlation in an anionic system, the need to combine continuum and discrete states, and the high number of degrees of freedom which make the

numerical calculation very cumbersome. Among the most popular computational methods for describing temporary anions, one can find a broad class of methods that compute the electron-scattering cross section (CS), such as the R-matrix method,[13] the Kohn method,[14] the Schwinger multichannel method,[15] or the formulation of a complex energy.[16] In the R-matrix method, the incoming electron described by a single-particle method collides with the n-particle target described with a configuration interaction type method, but the configuration space is necessarily quite small. Although such methods provide valuable information on CS, they essentially consist in static calculations and hence do not give much information about the dynamics of the attachment process and of the molecular dissociation. Dynamics can be followed through a real-time formalism, such as real-time TDDFT (Time-Dependent Density-Functional Theory).[17]

The prediction of resonant attachment energies can be investigated with much less cumbersome computational approaches. The so-called empirical correlation methods extrapolate an empirical correlation between experimental attachment energies and the corresponding energies calculated at *ab initio* level. Most often, a linear relationship is chosen as $E_{exp} = cE_{comp} + d$, where c and d are fitted parameters. Usually, E_{comp} is the energy of an unoccupied orbital obtained with a Hartree-Fock calculation for the neutral molecule. Such orbital energy is physically relevant for estimating the electron affinity of the molecule, and the linear fit can then be understood as a correction to the missing electron correlation effects.[18] Alternatively, in the Modelli's approach, E_{comp} refers to the energy of an unoccupied Kohn-Sham orbital.[12] These empirical methods can lead to a good estimation of the attachment energy in the case of shape resonances, while core-excited resonances are not accessible. At a higher level of calculation, e.g. with the linear response Equation-of-Motion Coupled-Cluster (EOM-CC) or TDDFT methods, the excitation energies of the anion (relative to the energy of the neutral molecule) can be used instead of the energies of virtual orbitals, and then the parameters c and d are expected to be closer to the ideal values of 1 and 0 respectively.[18] However, the determination of the empirical parameters c and d

requires the use of a large set of experimental data or high-level simulated values to serve as reference data, which limits the predictive nature of the methods. It is noteworthy that the scaling factor strongly depends on the level of theory (e.g. choices of the correlation method, the density functional, and the basis set), and possibly on the nature of molecules and excitations investigated. Consequently, several fits can be found in literature.[19–21]

One of the main issues to describe the electron scattering in the formalism of *ab initio* calculations is the difficulty to couple the continuum state of the incoming electron with the discrete states of the molecule. An elegant method to overcome this problem is the stabilization method, where the calculations are repeated using a varying simulation box size. The energies of discrete states, which correspond to the attachment of the electron, are expected to be independent of the box size. In contrast, the energies of continuum states which collapse for large boxes are found to strongly increase at relatively small box size due to the implicit confinement; such states are called discretized continuum (DC) states. The coupling of a discrete state of the molecule with a DC state leads to an avoided crossing in a so-called stabilization graph (plot of the electronic energies *vs* simulation box size). The resonance energy and the lifetime of the temporary anion can be extracted from the plateau.[16,18,22] Electronic calculations can be performed at EOM-MP2, EOM-CCSD, MRCI, ADC, or TDDFT level, while the simulation box is represented implicitly through a localized basis set whom diffuse exponents of Gaussian functions are scaled with a parameter α to increase or decrease the box size.[16,18,23–25]

In figure 1, we give a stabilization graph for CCl_2F_2 calculated at TDDFT level. Most of the calculated low-energy states are found to be DC states. They originate from transitions involving virtual orbitals that do not represent states localized on the molecule, but very far orbitals mainly developed on the most diffuse functions of the basis set. These continuum states can be discerned in plotting the energy of the virtual orbitals with respect to the α parameter ; the figure SI1 shows clearly the correspondence between virtual orbitals energies and energies of a free electron in a box (the so-called discretized continuum state). How-

ever, two avoided crossings are visible in Figure 1 (in the area marked with a circle). The corresponding excitation energies are calculated at 1.23 and 3.35 eV respectively.

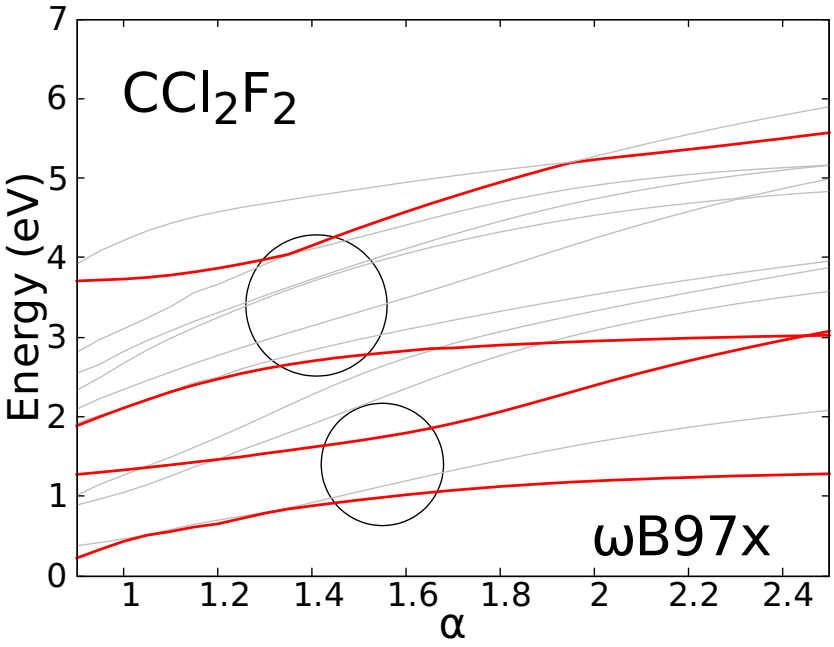

Figure 1: Stabilization graph for CCl_2F_2 using the TDDFT method with the ωB97x density functional[26] and the aug-cc-pvtz basis set.[27] The most diffuse s and p exponents are scaled by the α factor. The plot gives the lowest-energy excitations of the anion. States in light grey are DCs. Red lines highlight states involved in avoided crossings visible in areas marked with a circle.

While the stabilization method is one of the most efficient approach to investigate the electron attachment, calculations are not always easy due to a somewhat difficult choice of the basis set and the scaling process. Also, it is noteworthy that the analyses of the stabilization graph become difficult when several avoided crossings occur in a small energy range and involve several states. The resonant discrete state appears often to be an hybrid state mixing valence and continuum characters.

Here, we propose a simple approach to predict the resonance energies of the electron attachment using a TDDFT calculation and two different basis sets: a large basis set to compute the vertical electron affinity, and a smaller one to calculate the excitation energy of the anion. The present approach, in addition not to being cumbersome, does not calculate the intruder DC states.

One considers the attachment of a low-energy electron approaching a molecule with n electron. One denotes by ϵ the asymptotic kinetic energy of the incoming electron, and E_n the energy of the molecule in its ground state. Then, the whole $(n+1)$-electron system has a total energy of $\epsilon + E_n$, which actually corresponds to an excited state of the anion, and that can be computed at TDDFT level starting from the ground state of the $(n+1)$-electron system. From this value the vertical electron affinity must be subtracted to obtain the resonant attachment energy of the electron.

A schematic representation of our methodology of calculation is given in Figure 2. Calculations of the electron affinity and the excitation energy are distinct. First, the vertical electron affinity is calculated at DFT level as the difference of the total energy of the neutral and anionic species. The augmented correlation consistent valence triple-ζ + polarization basis set, aug-cc-pvtz,[27] which contains diffuse functions with low exponents, is used. Then, a TDDFT calculation for the anion is performed to obtain the excitation energy. For the latter, calculation is performed with the triple-ζ + polarization quality basis set, cc-pvtz,[27] which is well adapted for describing valence excitation states, i.e. states localized on the molecule. As this basis set does not contains any diffuse functions, the intruder DC states do not contaminate the spectrum of excited states (at least at low energy). Quadruple and quintuple ζ quality basis sets have been tried and did not change the calculated energies significantly. The vertical electron attachment energy is calculated as the sum of the vertical electron affinity (VEA) and the excitation energy. Of course, one must check that the SCF (Self-Consistent Field) procedure converges toward the same electronic state whatever the basis set, cc-pvtz or aug-cc-pvtz, is used. In some cases, one have had to replace an occupied orbital by a virtual one to get the correct electronic state.

Hybrid functionals were used as they are expected to be much more suitable than local functionals for calculating anions properties.[28] We have selected the range separated hybrid functional ωB97x[26] which contains an increasing amount of Hartree-Fock exchange at long range. It is particularly well adapted for computing excited states within the linear-response

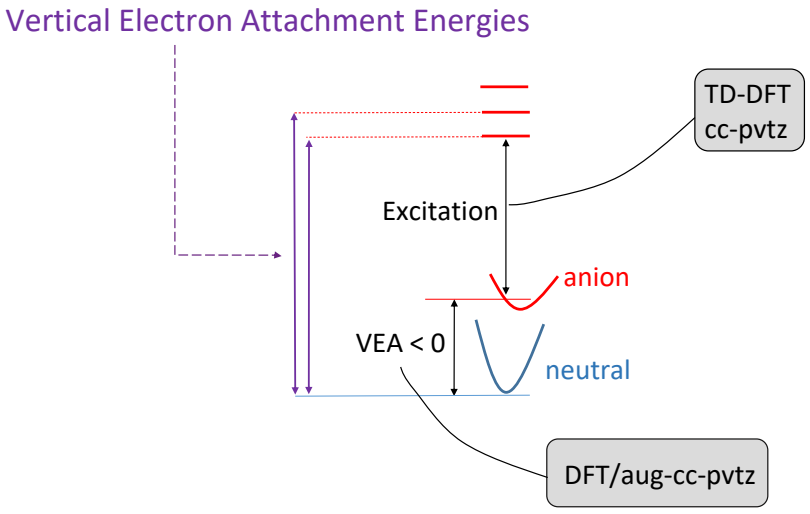

Figure 2: Schematic representation of the prediction of the vertical electron attachment energies. The vertical electron affinity (VEA) is calculated at DFT level using the large basis set aug-cc-pvtz, while the TDDFT excitations are computed with the non-augmented cc-pvtz basis set.

TDDFT formalism.[29] For comparison, we also present results using the density functional B3LYP,[30,31] and using the Coupled Cluster approach: CCSD(T)/aug-cc-pvtz level for calculating electron affinities and EOM-CCSD/cc-pvtz level for the excitation energies. All calculations were performed using the program Gaussian16.[32] Pre- and postprocessing operations were performed by using the graphical interface Gabedit.[33] The geometrical structure of the neutral molecules were optimized at ωB97x/cc-pvtz or B3LYP/cc-pvtz. The former were considered for Coupled Cluster calculations. The optimized structure of all molecules can be found in SI.

We have considered a set of 18 molecules (plotted in Figure SI2) for which experimental results of attachment energies are available from ETS or DEA measurements. The set contains 53 experimental resonances.

Vertical electron affinities (VEA) calculated at several levels are given in Table 1. VEA

is defined as

$$VEA = E_{neutral} - E_{anion}, \tag{1}$$

so that a negative VEA value means that the anion lies above the neutral molecule. A such anionic state is short lived, as it may suffer spontaneous electron detachment to the neutral ground state. Values obtained at ωB97x/aug-cc-pvtz level are found to be close to those calculated at CCSD(T)/aug-cc-pvtz level or measured in ETS (Table 1). As expected, calculations with the cc-pvtz basis set systematically underestimate the anion's energy. Interestingly, while B3LYP and ωB97x values are found to be close to each other when the small cc-pvtz basis set is used, they can give large differences in the provided values when the large aug-cc-pvtz basis set is used. B3LYP is unable to well estimate the anion when the VEA is very negative, i.e. when the anion is very unstable. For example, the B3LYP values of -0.49, -0.53, -0.56 eV for dichlorodifluoromethane, benzene, and furan respectively, are far from the ωB97x (-1.17, -1.58, -1.91 eV, respectively), CCSD(T) (-0.99, -1.62, -1.80 eV) and experimental data (-0.97, -1.12, -1.73 eV). Actually, B3LYP calculations overestimate the VEA due to a strong contribution of DC states, which lowers the energy of the negatively charged system when the basis set is large enough. Instead, the ωB97x potential, is able to lie a valence anionic state, and can furnish values close to those from CCSD(T) calculations.

The excitation energies of valence-type states of the anion were calculated using the non-augmented basis set cc-pvtz. This basis set were found to be large enough to treat anionic valence states. Table SI1 shows that energies calculated at ωB97x/cc-pvtz level compare well with those calculated with the augmented basis set (aug-cc-pvtz), and those obtained from the stabilization graph method. Using the cc-pvtz for the anionic excitation simplify significantly the analysis by unravelling far less states than with a more extended basis set. But an augmented basis set should be required when investigating the trapping of the electron via the long-range field of the molecule (e.g. dipole-bound anion), such anionic states are not considered in the present work.

Table 1: Calculated vertical electron affinities (VEA) compared to experimental data (ETS, except specified). For the chlorobenzene and butadiyne molecules, the B3LYP/aug-cc-pvtz calculations lead to DC states, instead of a valence anionic state.

molecule	B3LYP		ωB97x		CCSD(T)	Expt
	cc-pvtz	aug-cc-pvtz	cc-pvtz	aug-cc-pvtz	aug-cc-pvtz	
pyridine	-1.19	-0.48	-1.24	-1.00	-1.00	-0.59[a]
dichlorodifluoromethane	-1.24	-0.49	-1.75	-1.17	-0.99	-0.97[b]
chlorobenzene	-1.28	nc	-1.35	-1.15	-0.70	-0.72[c]
buta-1,3-diene	-1.16	-0.75	-1.30	-1.04	-0.79	-0.62[d]
benzonitrile	-0.23	-0.04	-0.35	-0.20	-0.32	-0.57[e]
p-benzoquinone	1.67	1.85	1.50	1.65	1.38	1.89[f]
benzene	-1.75	-0.53	-1.82	-1.58	-1.62	-1.12[g]
pyrazine	-0.54	-0.21	-0.58	-0.32	-0.02	-0.07[h]
nitrobenzene	0.57	0.84	0.36	0.60	0.41	
phenylacetylene	-0.71	-0.46	-0.86	-0.69	-0.50	-0.35[i]
furan	-2.38	-0.56	-2.54	-1.91	-1.80	-1.73[j]
nitromethane	-0.72	-0.02	-0.85	-0.38	-0.58	-0.45[k]
water	-2.91	-0.45	-3.34	-0.72	-0.61	
Benzaldehyde	0.05	0.25	-0.13	0.04	-0.42	> 0[l]
Phenyl isothiocyanate	-0.26	-0.74	-0.41	-0.26	-0.90	$>$ -0.2[m]
Butadiyne	-1.24	nc	-1.48	-1.16	-1.32	-1.00[n]
Cyanogen	0.05	0.26	-0.11	0.07	-0.31	-0.58[n]
$GeCl_4$	0.85	1.10	0.19	0.38	0.59	> 0[o]

[a] Ref[34] . [b] Ref[35] . [c] Ref[36] . [d] Ref[37] . [e] Ref[38] . [f] Adiabatic electron affinity, Ref[39] .
[g] Ref[34,40] .[h] Range of the vibrational broadening of 0.065-0.8 eV, Ref[41] . [i] Ref[42] .
[j] Ref[43,44] . [k] Ref[45] . [l] Ref[46] ; Adiabatic electron affinity = 0.35 eV[47] .
[m] DEA spectra, Ref[48,49] . [n] Ref[50] . [o] Ref[51] .

Calculated electron attachment energies are given in Table 2 at the high level ωB97x/MBS, where MBS stands for Mult-Basis-Set, i.e. a TDDFT calculation of the anion is performed with the cc-pvtz basis set while the electron affinity is evaluated with the large aug-cc-pvtz basis set following the schema presented in Figure 2. Results obtained with the less reliable ωB97x/cc-pvtz level, where cc-pvtz is used for both calculation steps, is also furnished for comparison, as well as the available experimental data. Figure 3 shows the good correlation between the DFT values and the experimental data. The reliability of our (TD-)DFT

calculations is estimated through the linear relationship

$$E_{exp} = mE_{calc} + b, \tag{2}$$

where E_{exp} and E_{calc} are the experimental and calculated resonance energies respectively, and m and b are fitted parameters. At ωB97x/MBS level, the values of $m = 0.976$ and $b = -0.246$, together with the root-mean-square deviation from the curve, rms=0.358, attest to the good performance, even though for some systems the agreement is not so good since the error can exceed 0.5 eV. But it is noteworthy that the experimental data may be subject to quite large error bars due to e.g. broadening of the resonances.

In order to judge the relevance of calculating excitation energies and vertical electron-affinities using two different basis sets, one can compare the results obtained with a multi basis-set (MBS) and using only cc-pvtz basis set. Doing so there is quite a difference in the coefficients obtained from the linear interpolation since $m = 0.829$, b = -0.124 eV and rms = 0.523 eV (Table 3, and Figure SI3), showing the systematic error made on the evaluation of the vertical electron affinity when a small basis set is used. Not only the correlation coefficient decreases, but also the deviation from the curve is more important. This comparison supports the need for an evaluation of the excitation energies and the vertical electron affinity using two different basis sets.

Performing calculations at B3LYP/MBS level gives the following coefficients: $m = 0.980$, $b = 0.191$ eV and rms = 0.464 eV (Tables 3 and SI1, Figures SI4-SI5). These results do not seem so different from the one obtained with the ωB97x functional, while the rms is larger with B3LYP. However, it is noteworthy that the quite good results using B3LYP originate from an error compensation occurring when we calculate the electron affinity (see above) and anionic excitations.

To evaluate the efficiency of the multi-basis-set ωB97x/MBS calculation, a comparison with Coupled-Cluster methods has been done for a restricted sample of 18 resonances (mainly

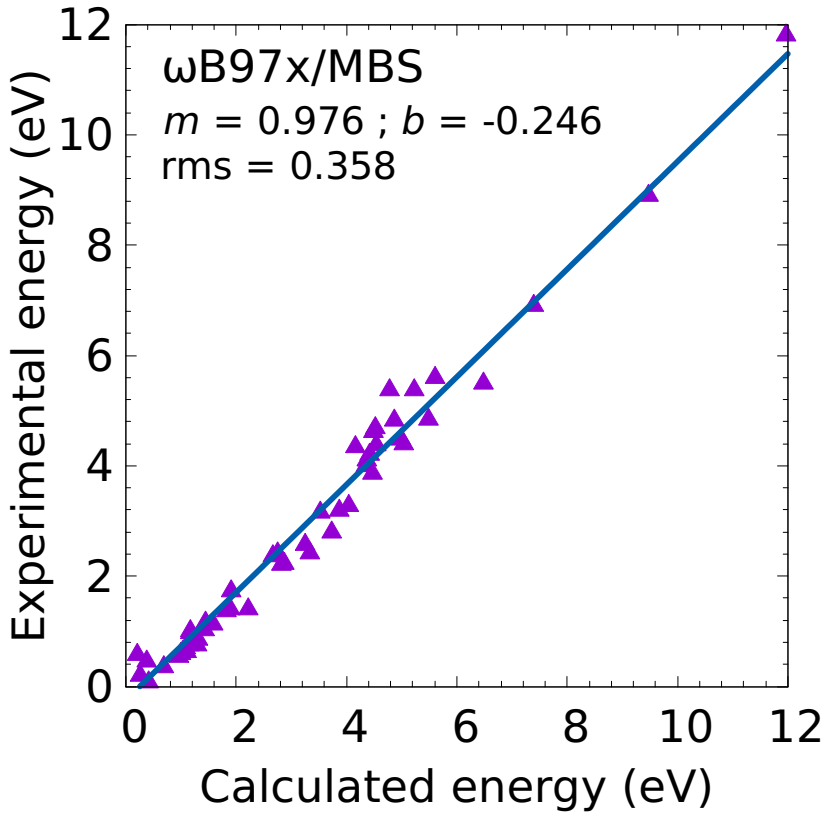

Figure 3: Electron attachment energy: comparison of the experimental data and the calculated ωB97X/MBS values.

due to the higher computational cost of the Coupled-Cluster methods). The EOM-CCSD method has been used with the cc-pvtz basis set to evaluate the anionic excitation energies while CCSD(T) with aug-cc-pvtz basis set has been used to evaluate the vertical electron affinities. As above, a linear fit of the data has been done and gave the following coefficient for Coupled-Cluster methods (Table 3, Figure SI6): $m = 0.900$, $b = 0.064$ eV and rms = 0.390 eV. For this reduced sample, with $m = 0.935$, b = -0.112 eV and rms = 0.379 eV, ωB97x/MBS performs as well as Coupled cluster. Previously, Sommerfeld[18] has calculated excitations and vertical electron-affinities using Coupled Cluster together with the cc-pvtz basis set on a large set of 63 states. He obtained a linear fit with $m = 0.857$, b = -0.387 and rms = 0.63 eV. These relative poorer results compared to ours shows once more that evaluating the vertical electron-affinity and the excitations with different basis sets is impor-

tant in order to accurately evaluate the vertical attachment energies. Of course, Coupled cluster calculations are expected to be improved using a higher quality basis set (e.g., 5-ζ or 6-ζ + more polarization functions), or by including corrections for the triple excitations as e.g. EOM-CC3, to evaluate excitation energies. But those calculations will be much more cumbersome than the present (TD-)DFT methodology.

Finally, the present methodology performed at ωB97x/MBS level furnishes very good results as they compare well with both calculated Coupled Clusters values and the experimental data obtained from electron transmission or DEA spectroscopies. However, it is noteworthy that the method should be used with caution: *(a)* one has to check that the augmented basis set calculation has converged to a valence state, *(b)* continuous states could, although happening rarely, appear in the non-augmented calculations, specially at high energy (> 10 eV), *(c)* the non-augmented basis set could in some cases give inaccurate excitation energies.

In conclusion, the method has proved to be an excellent compromise between computational efficiency and accuracy provided that an appropriate density functional is used. It allows to predict, at low computational cost, the resonance attachment energies of the electron in a valence state with a precision that competes to that of the cumbersome Coupled Cluster calculation. The method does not require any empirical parameters, and can treat both shape and core-excited resonances. The use of a large basis set (with diffuse functions) to compute the electron affinities results in accurate quantitative predictions, while the use of a less expanded basis set to obtain the anionic excitations prevents the occurrence of intruder discretized continuum states. In addition to give the resonance energies, the method could also furnish valuable interpretation of resonances by providing molecular orbitals in which the incoming electron is trapped, and possibly the electron-scattering cross section. This may lead to future work.

Notes

The authors declare no competing financial interests.

Acknowledgement

This work was performed using HPC resources from GENCI-IDRIS (Grant A0090807662) and the Pôle Scientifique de Modélisation Numérique (PSMN). It has received a financial support from the French National Research Agency (ANR-PRC BAMBI grant number 18-CE30-0009-03) and from CNRS MITI–"Défi ORIGINES 2020" (grant number 227617).

Supporting Information Available

The supporting information includes:

Table SI1: Excitation energies of the anion calculated at TDDFT/ωB97x level using the basis sets cc-pvtz, aug-cc-pvtz, and the stabilization graph method.

Table SI2: Comparison of attachment energies calculated at TDDFT/B3LYP and EOM-CCSD levels with experimental results.

Figure SI1: Plot of the energies of virtual orbitals of CCl_2F_2 relative to the scaling factor α.

Figure SI2: Molecules considered in the present investigation.

Figure SI3: Comparison of the experimental data and the calculated ωB97X/cc-pvtz values.

Figure SI4: Comparison of the experimental data and the calculated B3LYP/MBS values.

Figure SI5: Comparison of the experimental data and the calculated B3LYP/cc-pvtz values.

Figure SI6: Comparison of the experimental data and the calculated values obtained with ωB97x/MBS and EOM-CCSD/MBS.

Coordinates of optimized structures of molecules.

This information is available free of charge via the Internet at http://pubs.acs.org.

Table 2: Comparison of attachment energies calculated at TDDFT/ωB97x level with EOM-CCSD and experimental data.ωB97x/MBS stands for ωB97x/Multi-Basis-Set (TD(cc-pvtz) + VEA (aug-cc-pvtz)), while ωB97x/cc-pvtz refers to calculation performed using the cc-pvtz for both VEA and anionic excitations. EOM-CCSD/MBS means VEA calculated at CCSD(T)/aug-cc-pvtz level, and anionic excitation at EOM-CCSD/cc-pvtz level. EOM-CCSD/cc-pvtz means VEA calculated at CCSD(T)/cc-pvtz level, and anionic excitation at EOM-CCSD/cc-pvtz level.

molecule	ωB97x cc-pvtz	ωB97x MBS	EOM-CCSD cc-pvtz	EOM-CCSD MBS	Expt
pyridine	1.244	0.999	1.244	1.000	0.59[f]
C_5H_5N	1.684	1.439	1.755	1.512	1.16[f]
	5.227	4.982	5.474	5.230	4.48[f]
dichlorodifluoromethane	1.751	1.166	2.004	0.992	0.97[g]
CCl_2F_2	3.243	2.658	3.584	2.572	2.36[g]
	5.059	4.474	5.447	4.433	3.86[g]
chlorobenzene	1.350	1.149	1.555	0.703	0.75[h]
C_6H_5Cl	1.483	1.282	1.756	0.925	0.75[h]
	2.948	2.747	2.796	1.945	2.42[h]
	5.242	5.041	5.583	4.732	4.39[h]
buta-1,3-diene	1.298	1.039	1.298	0.786	0.62[e]
C_4H_6	3.946	3.725	3.946	3.352	2.8[e]
benzonitrile	0.347	0.201	0.623	0.323	0.57[d]
C_7H_5N	3.390	3.243	3.738	3.437	2.57[d]
	4.009	3.863	4.434	4.133	3.19[d]
	4.635	4.489	5.238	4.937	4.62[d]
p-benzoquinone	1.233	1.084			0.69[b]
$C_6H_4O_2$	2.034	1.885			1.41[b]
	4.681	4.532			4.37[b]
benzene	1.823	1.581			1.13[c]
C_6H_6	5.729	5.487			4.84[c]
pyrazine	0.580	0.321			0.07[a]
$C_4H_4N_2$	1.415	1.156			0.87[a]
	4.626	4.366			4.1[a]
nitrobenzene	1.200	0.967			0.55[j]
$C_6H_5NO_2$	3.271	1.826			1.36[j]
	4.757	4.524			4.69[j]
phenylacetylene	0.857	0.686			0.35[i]
C_8H_6	1.590	1.419			1.03[i]
	3.512	3.341			2.41[i]
	4.205	4.034			3.28[i]
	5.040	4.869			4.83[i]
Furan	2.538	1.909			1.73[l]
C_4H_4O	4.154	3.524			3.15[l]

Table 2 continued.

molecule	ωB97x cc-pvtz	ωB97x MBS	EOM-CCSD cc-pvtz	EOM-CCSD MBS	Expt
nitromethane	0.849	0.379			0.45[j]
CH_3NO_2	4.821	4.351			4.0[j]
water	10.025	7.399			6.9[k]
H_2O	12.093	9.467			8.9[k]
	14.588	11.962			11.8[k]
Benzaldehyde	1.481	1.313			0.85[m]
C_7H_6O	2.989	2.821			2.21[m]
	4.332	4.164			4.34[m]
Phenyl isothiocyanate	0.407	0.262			0.2[n]
C_7H_5NS	1.246	1.101			0.62[n]
	3.023	2.878			2.23[n]
	4.555	4.410			4.2[n]
Butadiyne	1.479	1.162	1.892	0.663	1.0[o]
$C4H_2$	5.926	5.609	6.312	5.084	5.6[o]
Cyanogen	0.108	-0.066	0.564	0.307	0.58[o]
C_2N_2	5.398	5.224	5.883	6.625	5.37[o]
germanium tetrachloride	-0.192	-0.379			0.0[p]
$GeCl_4$	2.395	2.209			1.4[p]
	6.676	6.490			5.5[p]

[a] Ref.[41] [b] Ref.[39] [c] Ref.[40] [d] Ref.[38] [e] Ref.[37] [f] Ref.[34,41] [g] Ref.[35] [h] Ref.[36] [i] Ref.[42] [j] Ref.[45] [k] Ref.[52] [l] Ref.[43,44] [m] Ref.[46] [n] Ref.[49] [o] Ref.[50] [p] Ref.[51]

Table 3: Parameters, m and b, for the linear fit (equation 2). rms stands for the root-mean-square deviation from the curve. ωB97x/MBS stands for ωB97x/Multi-Basis-Set (TD(cc-pvtz) + VEA (aug-cc-pvtz)). *Coupled Cluster: EOM-CCSD/cc-pvtz + VEA (CCSD(T)/aug-cc-pvtz). In the reduced sample, the number of states is reduced to 18 (instead of 53).

Method	m	b	rms
ωB97x/MBS	0.976	-0.246	0.358
B3LYP/MBS	0.980	0.191	0.464
ωB97x/cc-pvtz	0.829	-0.124	0.523
B3LYP/cc-pvtz	0.856	0.022	0.461
(reduced sample) Coupled Cluster*	0.900	0.064	0.390
(reduced sample) ωB97x/MBS	0.935	-0.112	0.379

References

(1) Boyer, M.; Rivas, N.; Tran, A.; Verish, C. The role of low-energy ($\leq$ 20eV) electrons in astrochemistry. *Surf. Sci.* **2016**, *652*, 26–32.

(2) Boudaiffa, B.; Cloutier, P.; Hunting, D.; Huels, M.; Sanche, L. Resonant formation of DNA strand breaks by low-energy (3 to 20eV) electrons. *Science* **2000**, *286*, 1658–1660.

(3) Sanche, L. Biological chemistry: beyond the radical thinking. *Nature* **2009**, *461*, 358–359.

(4) Sanche, L. In *Radiation Damage in Biomolecular Systems*; Gomez-Tejedor, G., Fuss, M., Eds.; Springer, 2012; Chapter 1, pp 3–43.

(5) Böhler, E.; Warneke, J.; Swiderek, P. Control of chemical reaction and synthesis by low-energy electron. *Chem. Soc. Rev.* **2013**, *42*, 9219–9231.

(6) Garcia, R.; Knoll, A.; Riedo, E. Advanced scanning probe lithography. *Nat. Nanotechnol.* **2014**, *9*, 577–587.

(7) Kopyra, J.; Rabilloud, F.; Abdoul-Carime, H. Core-excited resonances initiated by unusually low energies electron observed in dissociative electron attachment to Ni(II) (bis)acetylacetonate. *J. Chem. Phys.* **2020**, *153*, 124302.

(8) Abdoul-Carime, H.; Desfrançois, C. Electrons weakly bound to molecules by dipolar, quadrupolar or polarization forces. *Eur. Phys. J. D* **1998**, *2*, 149–156.

(9) Arumainayagam, C.; Lee, H.-L.; Nelson, R.; Haines, D.; Gunawardane, R. Low-energy electron-induced reactions in condensed matter. *Surf. Sci. Rep.* **2010**, *1*, 65.

(10) Pshenichnyuk, S. A.; Asfandiarov, N. L. Structural rearrangements as relaxation pathway for molecular negative ions formed via vibrational Feshbach resonance. *Phys. Chem. Chem. Phys.* **2020**, *22*, 16150.

(11) Sanche, L.; Schulz, G. J. Electron Transmission Spectroscopy: Rare Gases. *Phys. Rev. A* **1972**, *5*, 1672.

(12) Modelli, A. Electron attachment and intramolecular electron transfer in unsaturated chloroderivatives. *Phys. Chem. Chem. Phys.* **2003**, *5*, 2923–2930.

(13) Gorfinkiel, J.; Morgan, L.; Tennyson, J. Electron impact dissociative excitation of water within the adiabatic nuclei approximation. *J. Phys. B* **2002**, *35*, 543.

(14) McCurdy, C. W.; Rescigno, T. N.; Schneider, B. I. Interrelation between variational principles for scattering amplitudes and generalized R-matrix theory. *Phys. Rev. A* **1987**, *36*, 2061.

(15) Takatsuka, K.; Mckoy, V. Extension of the Schwinger variational principle beyond the static-exchange approximation. *Phys. Rev. A* **1981**, *24*, 2473.

(16) Falcetta, M. F.; DiFalco, L. A.; Ackerman, D. S.; Barlow, J. C.; Jordan, K. D. Assessment of Various Electronic Structure Methods for Characterizing Temporary Anion States: Application to the Ground State Anions of N_2, C_2H_2, C_2H_4, and C_6H_6. *J. Phys. Chem. A* **2014**, *118*, 7489–7497.

(17) Lacombe, L.; Dinh, P. H. M.; Reinhard, P.-G.; Suraud, E.; Sanche, L. Rare reaction channels in real-time time-dependent density functional theory: the test case of electron attachment. *Eur. Phys. J. D* **2015**, *69*, 195.

(18) Sommerfeld, T.; Weber, R. J. Empirical Correlation Methods for Temporary Anions. *J. Phys. Chem. A* **2011**, *115*, 6675–6682.

(19) Modelli, A.; Szepes, L. Electron attachment to the mixed dimers $(CH_3)3M\text{-}M'(CH_3)_3$, with M,M' = Si, Ge, Sn, and correlation with the calculated S^* virtual orbital energies. *Chem. Phys.* **2003**, *286*, 165–172.

(20) Kopyra, J.; Rabilloud, F.; Abdoul-Carime, H. Decomposition of Bis(acetylacetonate)zinc(II) by Slow Electrons. *Inorg. Chem.* **2020**, *59*, 12788–12792.

(21) Rabilloud, F.; Kopyra, J.; Abdoul-Carime, H. Fragmentation of Nickel(II) and Cobalt(II) Bis(acetylacetonate) Complexes Induced by Slow ($\leq$10 eV) Electrons. *Inorg. Chem.* **2021**, *60*, 8154–8163.

(22) Domcke, W. Theory of resonance and threshold effects in electron-molecule collisions: the projection-operator approach. *Phys. Report.* **1991**, *208*, 97–188.

(23) Cheng, H.-Y.; Chen, C.-W.; Huang, C.-H. Characterization of the Temporary Anion States on Perfluoroalkanes via Stabilized Koopmans' Theorem in Long-Range Corrected Density Functional Theory. *J. Phys. Chem. A* **2012**, *116*, 3224–3236.

(24) Cheng, H.-Y.; Huang, Y.-S. Temporary anion states of *p*-benzoquinone: shape and core-excited resonances. *Phys. Chem. Chem. Phys.* **2014**, *16*, 26306–26313.

(25) Cheng, H.-Y.; Lin, C.-J. Shape and core-excited resonances of thionucleobases. *Int. J. Quantum Chem.* **2018**, *118*, e25634.

(26) Chai, J.; Head-Gordon, M. Systematic optimization of long-range corrected hybrid density functionals. *J. Chem. Phys.* **2008**, *128*, 084106.

(27) Kendall, R. A.; Jr., T. H. D.; ; Harrison, R. J. Electron affinities of the first-row atoms revisited. Systematic basis sets and wave functions. *J. Chem. Phys.* **1992**, *96*, 6796–6806.

(28) Puiatti, M.; Mariano, D.; Vera, A.; Pierini, A. B. Species with negative electron affinity and standard DFT methods. Finding the valence anions. *Phys. Chem. Chem. Phys.* **2008**, *10*, 1394–1399.

(29) Rabilloud, F. Description of plasmon-like band in silver clusters: The importance of the long-range Hartree-Fock exchange in time-dependent density-functional theory simulations. *J. Chem. Phys.* **2014**, *141*, 144302.

(30) Becke, A. D. Density-functional thermochemistry. III. The role of exact exchange. *J. Chem. Phys.* **1993**, *98*, 5648–5652.

(31) Lee, C.; Yang, W.; Parr, R. G. Development of the Colle-Salvetti correlation-energy formula into a functional of the electron density. *Phys. Rev. B* **1988**, *37*, 785–789.

(32) Frisch, M. J.; Trucks, G. W.; Schlegel, H. B.; Scuseria, G. E.; Robb, M. A.; Cheeseman, J. R.; Scalmani, G.; Barone, V.; Petersson, G. A.; Nakatsuji, H. et al. Gaussian16 Revision C.01. 2016; Gaussian Inc. Wallingford CT.

(33) Allouche, A.-R. Gabedit A Graphical User Interface for Computational Chemistry Softwares. *J. Comput. Chem.* **2011**, *32*, 174–182.

(34) Burrow, P. D.; Ashe, A. J.; Bellville, D. J.; Jordan, K. D. Temporary anion states of phosphabenzene, arsabenzene, and stibabenzene. Trends in the π and π^* orbital energies. *J. Am. Chem. Soc.* **1982**, *104*, 425–429.

(35) Aflatooni, K.; Burrow, P. Dissociative electron attachment in chlorofluoromethanes and the correlation with vertical attachment energies. *Int. J. Mass Spectrom.* **2001**, *205*, 149–161.

(36) Modelli, A.; Venuti, M. Temporary π^* and σ^* Anions and Dissociative Electron Attachment in Chlorobenzene and Related Molecules. *J. Phys. Chem. A* **2001**, *105*, 5836–5841.

(37) Burrow, P.; Jordan, K. On the electron affinities of ethylene and 1,3-butadiene. *Chemical Physics Letters* **1975**, *36*, 594–598.

(38) Burrow, P. D.; Howard, A. E.; Johnston, A. R.; Jordan, K. D. Temporary anion states of

hydrogen cyanide, methyl cyanide, and methylene dicyanide, selected cyanoethylenes, benzonitrile, and tetracyanoquinodimethane. *J. Phys. Chem.* **1992**, *96*, 7570–7578.

(39) Modelli, A.; Burrow, P. D. Electron transmission study of the negative ion states of p-benzoquinone, benzaldehyde, and related molecules. *J. Phys. Chem.* **1984**, *88*, 3550–3554.

(40) Burrow, P. D.; Michejda, J. A.; Jordan, K. D. Electron transmission study of the temporary negative ion states of selected benzenoid and conjugated aromatic hydrocarbons. *J. Chem. Phys.* **1987**, *86*, 9–24.

(41) Nenner, I.; Schulz, G. J. Temporary negative ions and electron affinities of benzene and N-heterocyclic molecules: pyridine, pyridazine, pyrimidine, pyrazine, and s-triazine. *J. Chem. Phys.* **1975**, *62*, 1747–1758.

(42) Scheer, A. M.; Burrow, P. D. π^* Orbital System of Alternating Phenyl and Ethynyl Groups: Measurements and Calculations. *J. Phys. Chem. B* **2006**, *110*, 17751–17756.

(43) Sulzer, P.; Ptasinska, S.; Zappa, F.; Mielewska, B.; Milosavljevic, A. R.; Scheier, P.; Märk, T. D.; Bald, I.; Gohlke, S.; Huels, M. A. et al. Dissociative electron attachment to furan, tetrahydrofuran, and fructose. *J. Chem. Phys.* **2006**, *125*.

(44) Modelli, A.; Burrow, P. D. Electron Attachment to the Aza-Derivatives of Furan, Pyrrole, and Thiophene. *J. Phys. Chem. A* **2004**, *108*, 5721–5726.

(45) Modelli, A.; Venuti, M. Empty level structure and dissociative electron attachment in gas-phase nitro derivatives. *Int. J. Mass Spectrom.* **2001**, *205*, 7–16.

(46) Ameixa, J.; Arthur-Baidoo, E.; da Silva, J. P.; Ryszka, M.; Carmichael, I.; Cornetta, L. M.; do N. Varella, M. T.; da Silva, F. F.; Ptasińska, S.; Denifl, S. Formation of resonances and anionic fragments upon electron attachment to benzaldehyde. *Phys. Chem. Chem. Phys.* **2020**, *22*, 8171–8181.

(47) Buonaugurio, A.; Zhang, X.; Stokes, S. T.; Wang, Y.; Ellison, G. B.; Bowen, K. H. The photoelectron spectrum of the benzaldehyde anion. *Int. J. Mass. Spectro.* **2015**, *377*, 278–280.

(48) Modelli, A.; Jones, D. Temporary Anion States and Dissociative Electron Attachment to Isothiocyanates. *J. Phys. Chem. A* **2006**, *110*, 13195–13201.

(49) Pshenichnyuk, S. A.; Rakhmeyev, R. G.; Asfandiarov, N. L.; Komolov, A. S.; Modelli, A.; Jones, D. Can the Electron-Accepting Properties of Odorants Be Involved in Their Recognition by the Olfactory System? *J. Phys. Chem. Lett.* **2018**, *9*, 2320–2325.

(50) Ng, L.; Balaji, V.; Jordan, K. Measurement of the vertical electron affinities of cyanogen and 2,4-hexadiyne. *Chemical Physics Letters* **1983**, *101*, 171–176.

(51) Kumar, T. P. R.; Brynjarsson, B.; Òmarsson, B.; Hoshino, M.; Tanaka, H.; Limão-Vieira, P.; Jones, D.; Brunger, M. J.; Ingòlfsson, O. Negative ion formation through dissociative electron attachment to the group IV tetrachlorides: Carbon tetrachloride, silicon tetrachloride and germanium tetrachloride. *Int. J. Mass Spectrom.* **2018**, *426*, 12–28.

(52) Fedor, J.; Cicman, P.; Coupier, B.; Feil, S.; Winkler, M.; Głuch, K.; Husarik, J.; Jaksch, D.; Farizon, B.; Mason, N. J. et al. Fragmentation of transient water anions following low-energy electron capture by H2O/D2O. *J. Phys. B: At. Mol. Opt. Phys.* **2006**, *39*, 3935–3944.

Multi-Basis-Set (TD-)DFT Methods for Predicting Electron Attachment Energies

Supporting Information

Guillaume Thiam* and Franck Rabilloud*

Université de Lyon, Université Claude Bernard Lyon 1, CNRS, Institut Lumière Matière, UMR5306, F-69622 Villeurbanne, France

E-mail: guillaume.thiam@univ-lyon1.fr; franck.rabilloud@univ-lyon1.fr

Supporting information:

Table SI1: Excitation energies of the anion calculated at TDDFT/ωB97x level using the basis sets cc-pvtz, aug-cc-pvtz, and the stabilization graph method.

Table SI2: Comparison of attachment energies calculated at TDDFT/B3LYP and EOM-CCSD levels with experimental results.

Figure SI1: Plot of the energies of virtual orbitals of CCl_2F_2 relative to the scaling factor α.

Figure SI2: Molecules considered in the present investigation.

Figure SI3: Comparison of the experimental data and the calculated ωB97x/cc-pvtz values.

Figure SI4: Comparison of the experimental data and the calculated B3LYP/MBS values.

Figure SI5: Comparison of the experimental data and the calculated B3LYP/cc-pvtz values.

Figure SI6: Comparison of the experimental data and the calculated values obtained with ωB97x/MBS and EOM-CCSD/MBS.

Coordinates of optimized structures of molecules.

Tables

Table SI1: Excitation energies of the anion calculated at TDDFT/ωB97x level. [a]When two values are given for ωB97x/aug-cc-pvtz, they correspond to the energies of a valence state and a continuum state which are involved in an avoided crossing visible in the stabilization graph. [b]The stabilization graph method is performed with the basis set aug-cc-pvtz where the most diffuse exponents are scaled by a factor $\alpha = 0.5 - 3$.

molecule	ωB97x/cc-pvtz	ωB97x/aug-cc-pvtz[a]	Stabilization method[b]
Pyridine	0.44	0.46	
	3.98	4.05	
Dichlorodifluoromethane	1.49	0.46 ; 1.05	1.25
	3.31	2.11 ; 3.75	3.35
Chlorobenzene	0.13	0.10	0.12
	1.60	1.41 ; 2.10	2.19
	3.89	3.52 ; 3.79	3.79
	4.25	4.05	4.23
Buta-1,3-diene	2.65	1.42 ; 2.21	2.16
Benzonitrile	0.76	0.72	0.73
	3.04	2.75	3.01
	3.66	3.24	3.50
	4.63	4.25	4.28
p-benzoquinone	2.73	2.67	
	3.53	3.36	
	6.18	6.27	
Benzene	3.91	4.15	
Pyrazine	0.84	0.90	
	4.05	4.08	
Nitrobenzene	1.56	1.65	
	2.42	2.34	
	5.12	5.10	
Phenylacetylene	0.73	0.70	0.70
	2.66	2.65	2.46
	3.35	3.07	3.14
	4.18	4.15	4.13
Furan	1.62	1.43	
Nitromethane	3.97	2.77	3.33
Water	6.68	7.60	7.07
	8.75	9.32	9.23
	11.24	9.46	11.81
Benzaldehyde	1.36	1.31	
	2.86	2.80	
	4.21	4.19	
Phenyl-isothiocyanate	0.84	0.79	
	2.62	2.38	
	4.15	4.07	
Butadiyne	4.45	4.64	4.38

Table SI1 continued.

molecule	ωB97x/cc-pvtz	ωB9/aug-cc-pvtz[a]	Stabilization method[b]
Cyanogene	5.30	5.19	5.24
$GeCl_4$	2.59	2.53	
	6.87	6.67	

Table SI2: Comparison of attachment energies calculated at TDDFT/B3LYP and EOM-CCSD levels with experimental results. EOM-CCSD/MBS means vertical electron affinity (VEA) calculated at CCSD(T)/aug-cc-pvtz level, and anionic excitation at EOM-CCSD/cc-pvtz level. EOM-CCSD/cc-pvtz means vertical electron affinity (VEA) calculated at CCSD(T)/cc-pvtz level, and anionic excitations at EOM-CCSD/cc-pvtz level. B3LYP/MBS stands for B3LYP/Multi-Basis-Set (TD(cc-pvtz) + VEA (aug-cc-pvtz)).

molecule	B3LYP cc-pvtz	B3LYP MBS	EOM-CCSD cc-pvtz	EOM-CCSD MBS	Expt
pyridine	1.186	0.479	1.244	1.000	0.59[f]
C_5H_5N	1.582	0.875	1.755	1.512	1.16[f]
	5.149	4.442	5.474	5.230	4.48[f]
dichlorodifluoromethane	1.241	0.492	2.004	0.992	0.97[g]
CCl_2F_2	3.009	2.261	3.584	2.572	2.36[g]
	4.692	3.944	5.447	4.433	3.86[g]
chlorobenzene	1.280		1.555	0.703	0.75[h]
C_6H_5Cl	1.395		1.756	0.925	0.75[h]
	2.847		2.796	1.945	2.42[h]
	5.069		5.583	4.732	4.39[h]
buta-1,3-diene	1.155	0.748	1.298	0.786	0.62[e]
C_4H_6	3.840	3.433	3.946	3.352	2.8[e]
benzonitrile	0.231	0.040	0.623	0.323	0.57[d]
C_7H_5N	3.723	3.539	3.738	3.437	2.57[d]
	4.018	3.827	4.343	4.133	3.19[d]
	4.461	4.278	5.238	4.937	4.62[d]

Table SI2 continued.

molecule	B3LYP cc-pvtz	B3LYP MBS	EOM-CCSD cc-pvtz	EOM-CCSD MBS	Expt
p-benzoquinone	0.863	0.692			0.69[b]
$C_6H_4O_2$	1.695	1.524			1.41[b]
	4.615	4.444			4.37[b]
benzene	1.750	0.445			1.13[c]
C_6H_6	5.568	4.263			4.84[c]
pyrazine	0.543	0.214			0.07[a]
$C_4H_4N_2$	1.305	0.975			0.87[a]
	4.611	3.444			4.1[a]
nitrobenzene	0.624	0.362			0.55[j]
$C_6H_5NO_2$	1.945	1.683			1.36[j]
	4.415	4.153			4.69[j]
phenylacetylene	0.711	0.455			0.35[i]
C_8H_6	1.373	1.117			1.03[i]
	2.739	2.482			2.41[i]
	3.901	3.644			3.28[i]
	4.881	4.625			4.83[i]
Furan	2.377	0.559			1.73[l]
C_4H_4O	3.988	2.170			3.15[l]
nitromethane	0.719	0.017			0.45[j]
CH_3NO_2	4.048	3.346			4.0[j]
water	9.113	6.645			6.9[k]
H_2O	10.759	8.291			8.9[k]
	14.177	11.709			11.8[k]
Benzaldehyde	1.083	0.883			0.85[m]
C_7H_6O	2.839	2.640			2.21[m]
	4.162	3.962			4.34[m]
Phenyl isothiocyanate	0.259	0.074			0.2[n]
C_7H_5NS	0.946	0.761			0.62[n]
	2.909	2.724			2.23[n]
	4.372	4.187			4.2[n]
Butadiyne	1.237		1.892	0.663	1.0[o]
$C4H_2$	5.603		6.312	5.084	5.6[o]
Cyanogen	-0.046	-0.261	0.564	0.307	0.58[o]
C_2N_2	4.974	4.759	5.883	5.625	5.37[o]
germanium tetrachloride	-0.854	-1.09			0.0[p]
$GeCl_4$	2.069	1.824			1.4[p]
	5.523	5.278			5.5[p]

[a] Ref[1] . [b] Ref[2] . [c] Ref[3] . [d] Ref[4] . [e] Ref[5] . [f] Ref[1,6] . [g] Ref[7] . [h] Ref[8] . [i] Ref[9] . [j] Ref[10] . [k] Ref[11] . [l] Ref[12,13] . [m] Ref[14] . [n] Ref[15] . [o] Ref[16] . [p] Ref[17] .

Figures

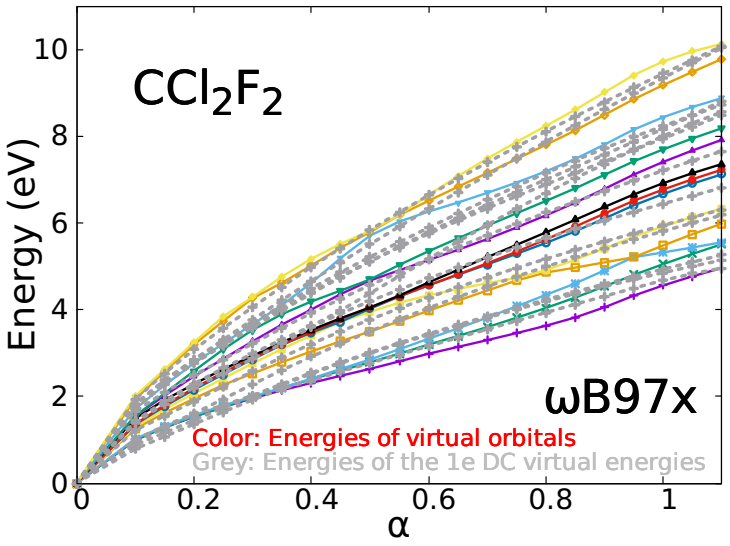

Figure SI1: Plot of the energies of virtual orbitals of CCl_2F_2 relative to the scaling factor α. Grey lines are the energies of one free electron in the absence any charges (nuclear and electrons) calculated at the same level of calculation (ωB97x) with the same molecular basis set as that used for the molecule. The clear correspondence between energies shows that virtual orbitals of the molecule represent some discretized continuum states (as a "free" electron in a box) when the basis set is enough extended (i.e. small values of α).

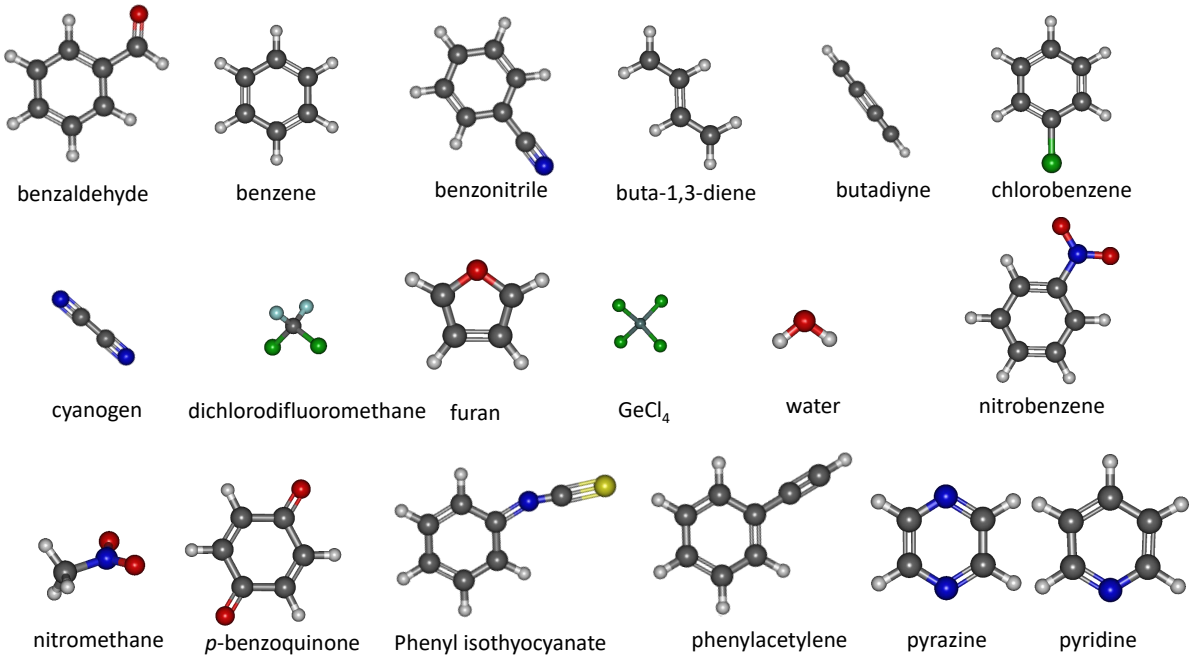

Figure SI2: Molecules considered in the present investigation.

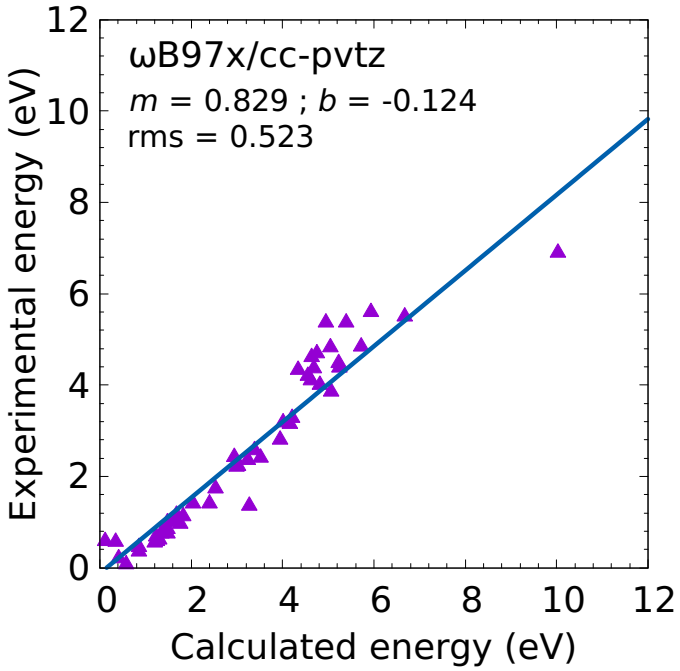

Figure SI3: Comparison of the experimental data and the calculated ωB97x/cc-pvtz values.

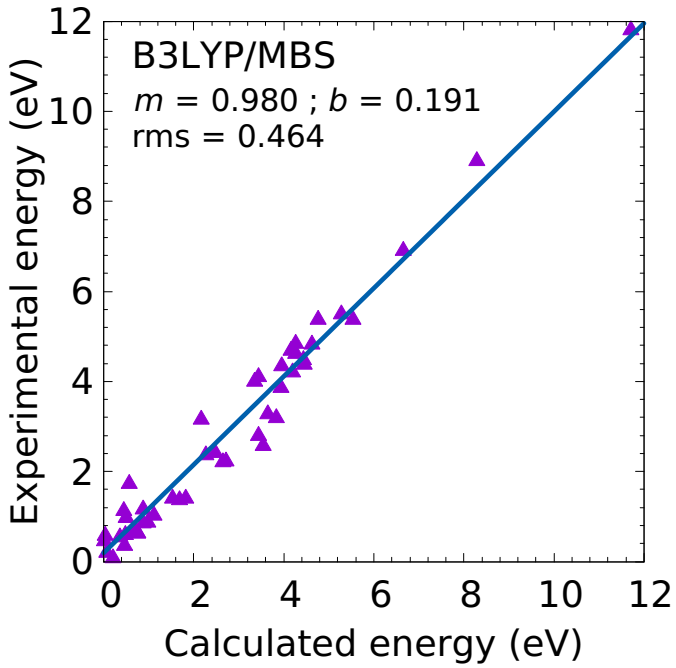

Figure SI4: Comparison of the experimental data and the calculated B3LYP/MBS values.

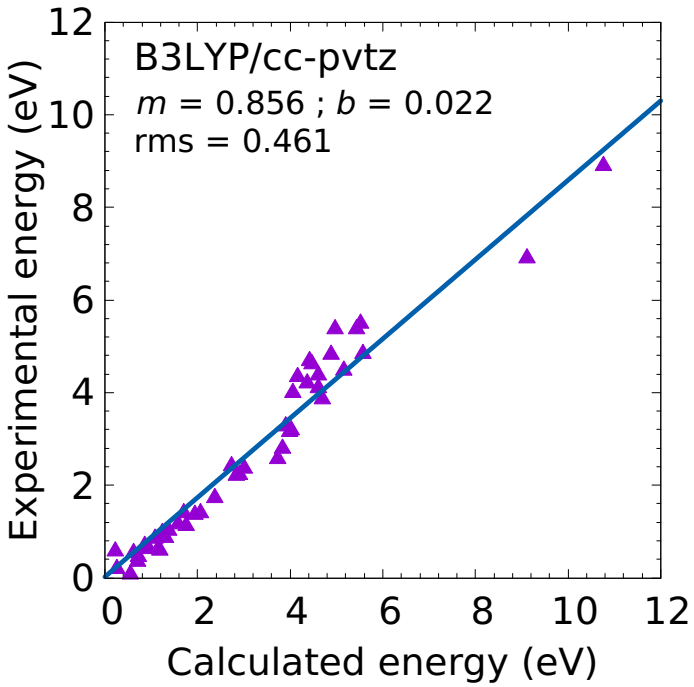

Figure SI5: Comparison of the experimental data and the calculated B3LYP/cc-pvtz values.

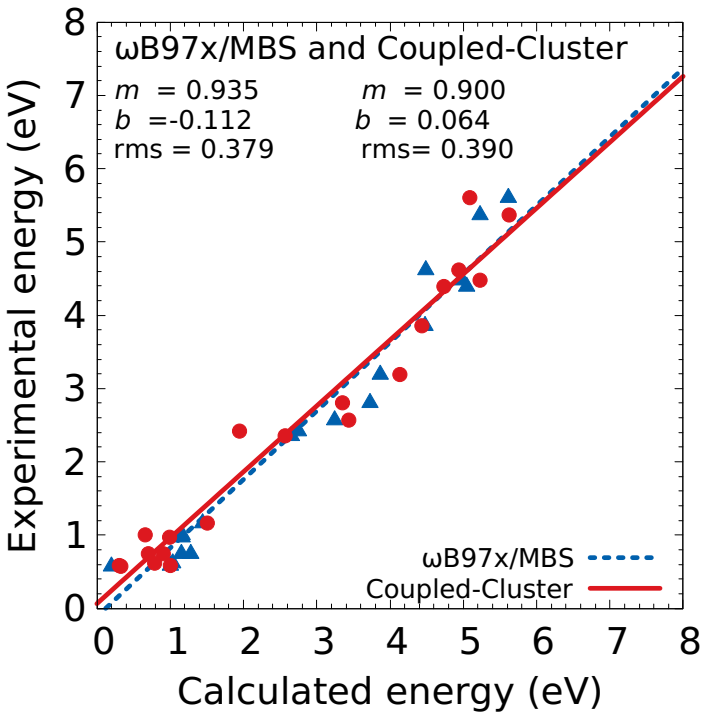

Figure SI6: Comparison of the experimental data and the calculated value obtained with ωB97x/MBS and EOM-CCSD/MBS (electron affinity (VEA) calculated at CCSD(T)/aug-cc-pvtz level, and anionic excitations at EOM-CCSD/cc-pvtz level).

References

(1) Nenner, I.; Schulz, G. J. Temporary negative ions and electron affinities of benzene and N-heterocyclic molecules: pyridine, pyridazine, pyrimidine, pyrazine, and s-triazine. *J. Chem. Phys.* **1975**, *62*, 1747–1758.

(2) Modelli, A.; Burrow, P. D. Electron transmission study of the negative ion states of p-benzoquinone, benzaldehyde, and related molecules. *J. Phys. Chem.* **1984**, *88*, 3550–3554.

(3) Burrow, P. D.; Michejda, J. A.; Jordan, K. D. Electron transmission study of the temporary negative ion states of selected benzenoid and conjugated aromatic hydrocarbons. *J. Chem. Phys.* **1987**, *86*, 9–24.

(4) Burrow, P. D.; Howard, A. E.; Johnston, A. R.; Jordan, K. D. Temporary anion states of hydrogen cyanide, methyl cyanide, and methylene dicyanide, selected cyanoethylenes, benzonitrile, and tetracyanoquinodimethane. *J. Phys. Chem.* **1992**, *96*, 7570–7578.

(5) Burrow, P.; Jordan, K. On the electron affinities of ethylene and 1,3-butadiene. *Chemical Physics Letters* **1975**, *36*, 594–598.

(6) Burrow, P. D.; Ashe, A. J.; Bellville, D. J.; Jordan, K. D. Temporary anion states of phosphabenzene, arsabenzene, and stibabenzene. Trends in the π and π^* orbital energies. *J. Am. Chem. Soc.* **1982**, *104*, 425–429.

(7) Aflatooni, K.; Burrow, P. Dissociative electron attachment in chlorofluoromethanes and the correlation with vertical attachment energies. *Int. J. Mass Spectrom.* **2001**, *205*, 149–161.

(8) Modelli, A.; Venuti, M. Temporary π^* and σ^* Anions and Dissociative Electron Attachment in Chlorobenzene and Related Molecules. *J. Phys. Chem. A* **2001**, *105*, 5836–5841.

(9) Scheer, A. M.; Burrow, P. D. π^* Orbital System of Alternating Phenyl and Ethynyl Groups: Measurements and Calculations. *J. Phys. Chem. B* **2006**, *110*, 17751–17756.

(10) Modelli, A.; Venuti, M. Empty level structure and dissociative electron attachment in gas-phase nitro derivatives. *Int. J. Mass Spectrom.* **2001**, *205*, 7–16.

(11) Fedor, J.; Cicman, P.; Coupier, B.; Feil, S.; Winkler, M.; Głuch, K.; Husarik, J.; Jaksch, D.; Farizon, B.; Mason, N. J.; Scheier, P.; Märk, T. D. Fragmentation of transient water anions following low-energy electron capture by H2O/D2O. *J. Phys. B: At. Mol. Opt. Phys.* **2006**, *39*, 3935–3944.

(12) Sulzer, P.; Ptasinska, S.; Zappa, F.; Mielewska, B.; Milosavljevic, A. R.; Scheier, P.; Märk, T. D.; Bald, I.; Gohlke, S.; Huels, M. A.; Illenberger, E. Dissociative electron attachment to furan, tetrahydrofuran, and fructose. *J. Chem. Phys.* **2006**, *125*.

(13) Modelli, A.; Burrow, P. D. Electron Attachment to the Aza-Derivatives of Furan, Pyrrole, and Thiophene. *J. Phys. Chem. A* **2004**, *108*, 5721–5726.

(14) Ameixa, J.; Arthur-Baidoo, E.; da Silva, J. P.; Ryszka, M.; Carmichael, I.; Cornetta, L. M.; do N. Varella, M. T.; da Silva, F. F.; Ptasińska, S.; Denifl, S. Formation of resonances and anionic fragments upon electron attachment to benzaldehyde. *Phys. Chem. Chem. Phys.* **2020**, *22*, 8171–8181.

(15) Pshenichnyuk, S. A.; Rakhmeyev, R. G.; Asfandiarov, N. L.; Komolov, A. S.; Modelli, A.; Jones, D. Can the Electron-Accepting Properties of Odorants Be Involved in Their Recognition by the Olfactory System? *J. Phys. Chem. Lett.* **2018**, *9*, 2320–2325.

(16) Ng, L.; Balaji, V.; Jordan, K. Measurement of the vertical electron affinities of cyanogen and 2,4-hexadiyne. *Chemical Physics Letters* **1983**, *101*, 171–176.

(17) Kumar, T. P. R.; Brynjarsson, B.; Òmarsson, B.; Hoshino, M.; Tanaka, H.; Limão-Vieira, P.; Jones, D.; Brunger, M. J.; Ingòlfsson, O. Negative ion formation through

dissociative electron attachment to the group IV tetrachlorides: Carbon tetrachloride, silicon tetrachloride and germanium tetrachloride. *Int. J. Mass Spectrom.* **2018**, *426*, 12–28.

xyz coordinates of all molecules.

Benzene

C -1.201551 0.693471 0.000000

C 0.000000 1.387223 -0.000000

C -1.201456 -0.693614 0.000000

C 1.201449 -0.693639 -0.000000

C 1.201359 0.693790 -0.000000

C 0.000193 -1.387227 0.000000

H -2.139134 1.235063 0.000000

H 0.000026 -2.469986 0.000000

H 2.139073 1.235146 -0.000000

H -2.138943 -1.235372 0.000000

H -0.000234 2.469986 -0.000000

H 2.139248 -1.234860 -0.000000

P-Benzoquinone

C -1.269287 0.664550 -0.000000

C -0.000008 1.436831 -0.000000

C -1.269281 -0.664487 0.000000

C 1.269308 -0.664552 0.000000

C 1.269308 0.664492 -0.000000

C -0.000008 -1.436834 0.000000

H -2.178028 1.252902 -0.000000

H 2.178103 1.252781 -0.000000

H -2.178082 -1.252768 0.000000

H 2.178044 -1.252916 0.000000

O -0.000040 -2.646417 0.000000

O 0.000011 2.646417 -0.000000

Benzonitrile

C -1.208460 -0.090670 0.000000

C 0.000000 0.600970 0.000000

C -1.203394 -1.474555 0.000000

C 1.202746 -1.474954 0.000000

C 1.208254 -0.091063 0.000000

C -0.000440 -2.165829 0.000000

C 0.000453 2.038402 0.000000

H -2.139583 0.459856 0.000000

H -0.000656 -3.248151 0.000000

H 2.139535 0.459197 0.000000

H -2.140722 -2.014881 0.000000

H 2.139910 -2.015555 0.000000

N 0.000937 3.186533 0.000000

Buta-1,3-diene

C 1.101969 -1.470278 0.000000

C -0.000082 -0.730451 0.000000

C -0.000000 0.730247 -0.000000

C -1.101933 1.470445 -0.000000

H 2.084991 -1.013269 0.000000

H 1.060264 -2.551073 0.000000

H -0.973533 -1.212582 0.000000

H 0.973588 1.212142 -0.000000

H -2.085098 1.013727 -0.000000

H -1.059940 2.551277 -0.000000

Pyridine

C 0.071213 1.363071 0.000000

C 1.212809 0.576495 0.000000

C 0.000000 -1.342808 0.000000

C -1.200656 -0.649305 0.000000

C -1.162910 0.734817 0.000000

H 0.153011 2.441695 0.000000

H -2.139629 -1.186384 0.000000

H 2.195360 1.037065 0.000000

H 0.005494 -2.427955 0.000000

H -2.078101 1.313372 0.000000

N 1.191590 -0.753060 0.000000

Nitrobenzene

C 0.000676 -2.500823 0.000000

C -1.203613 -1.811351 0.000000

C 1.204800 -1.810755 0.000000

C -0.000000 0.238489 0.000000

C -1.211826 -0.426380 0.000000

C 1.212263 -0.425959 0.000000

H 0.000963 -3.583181 0.000000

H 2.131011 0.141580 0.000000

H -2.131022 0.140355 0.000000

H 2.141630 -2.351617 0.000000

H -2.140302 -2.352459 0.000000

N -0.000512 1.715447 0.000000

O -1.073913 2.275700 0.000000

O 1.072351 2.276533 0.000000

nitromethane

C 0.039005 -1.313541 0.000000

N 0.000000 0.173418 0.000000

O 1.055279 0.763853 0.000000

O -1.096211 0.685087 0.000000

H -0.490769 -1.647326 0.887216

H 1.074971 -1.629545 0.000000

H -0.490769 -1.647326 -0.887216

Benzaldehyde

C 0.583599 -2.139008 0.000000

C -0.741064 -1.715535 -0.000000

C 1.616162 -1.213838 0.000000

C 0.000000 0.566986 0.000000

C -1.033951 -0.364886 -0.000000

C 1.321905 0.140727 0.000000

H 0.809829 -3.197869 0.000000

H 2.120343 0.874850 0.000000

H -2.055656 -0.006759 -0.000000

H 2.645517 -1.547823 0.000000

H -1.541255 -2.444318 -0.000000

C -0.299104 2.017299 -0.000000

O -1.407149 2.487014 -0.000000

H 0.593125 2.675340 0.000000

Butadyine

C 0.000000 0.000000 1.887688

C 0.000000 0.000000 0.690021

C 0.000000 0.000000 -0.690021

C 0.000000 0.000000 -1.887688

H 0.000000 0.000000 2.951266

H 0.000000 0.000000 -2.951266

Cyanogene

C 0.000000 0.000000 0.693935

C 0.000000 0.000000 -0.693935

N 0.000000 0.000000 1.840605

N 0.000000 0.000000 -1.840605

Phenylacetylene (C8H6)

C -0.000000 0.583484 0.000000

C -1.203973 -0.119978 0.000000

C 1.204027 -0.119779 0.000000

C 0.000195 -2.198931 0.000000

C -1.200658 -1.504258 0.000000

C 1.200909 -1.504101 0.000000

C -0.000179 2.018937 0.000000

C -0.000291 3.216419 0.000000

H -0.000796 4.279643 0.000000

H 2.139741 -2.042748 0.000000

H -2.139387 -2.043083 0.000000

H 2.136880 0.428538 0.000000

H -2.136874 0.428256 0.000000

H 0.000255 -3.281361 0.000000

Pyrazine

C -0.000000 1.322252 0.000000

C 1.180953 0.594758 0.000000

C 0.000150 -1.322257 -0.000000

C -1.181023 -0.594627 -0.000000

H 0.015471 2.406398 0.000000

H -2.142222 -1.096366 -0.000000

H 2.142244 1.096277 0.000000

H -0.015553 -2.406418 -0.000000

N -1.189629 0.732794 -0.000000

N 1.189569 -0.732886 0.000000

Dichlorodifluromethane

C 0.000003 0.337152 -0.000012

Cl -1.455130 -0.651288 -0.000035

Cl 1.455134 -0.651283 -0.000044

F 0.000007 1.117696 1.075261

F -0.000016 1.117949 -1.075102

Chlorobenzene

C 0.000865 -2.256274 -0.000000

C -1.199166 -1.561087 -0.000000

C 1.200177 -1.560497 -0.000000

C -0.000000 0.503198 0.000000

C -1.207034 -0.174561 -0.000000

C 1.207176 -0.173639 0.000000

H 0.000989 -3.338360 -0.000000

H 2.135959 0.379809 0.000000

H -2.135957 0.378650 -0.000000

H 2.140180 -2.097013 -0.000000

H -2.138621 -2.098563 -0.000000

Cl -0.000862 2.241920 0.000000

Water

O 0.000000 0.000000 0.117043

H 0.000000 0.757944 -0.468173

H 0.000000 -0.757944 -0.468173

Furan

C 0.690922 -0.970306 0.000000

C -0.657659 -0.931473 0.000000

C 1.124201 0.394308 0.000000

C 0.000000 1.140150 0.000000

O -1.097902 0.348454 0.000000

H 1.305485 -1.854614 0.000000

H -0.183990 2.200465 0.000000

H -1.419343 -1.691802 0.000000

H 2.136280 0.762243 0.000000

Phenyl-isothiocyanate

C 3.180075 0.262326 0.000132

C 2.689691 -1.035018 0.000165

C 2.298447 1.333935 0.000096

C 0.448917 -0.188646 0.000122

C 1.324800 -1.267163 0.000163

C 0.931766 1.116715 0.000093

H 4.247525 0.438922 0.000135

H 0.234015 1.943495 0.000066

H 0.926255 -2.272428 0.000192

H 2.676333 2.348028 0.000071

H 3.373295 -1.873875 0.000193

N -0.916289 -0.423953 0.000119

C -2.064314 -0.156006 -0.000138

S -3.618731 0.124167 -0.000331

GeCl4

Ge -0.000101 0.000027 -0.000064

Cl -1.621947 1.114832 -0.767542

Cl -0.711916 -1.824293 0.792143

Cl 0.954943 1.105465 1.525845

Cl 1.379109 -0.396054 -1.550325